PLOS ONE

The endocytic receptor protein LRP-1 modulate P-glycoprotein mediated drug resistance in MCF-7 cells

Aubery Henry[1‡], Marine Mauperin[1‡], Jerome Devy[1], Stephane Dedieu[1], Lise Chazee[1], Cathy Hachet[1], Christine Terryn[2], Laurent Duca[1], Laurent Martiny[1], Emmanuelle Devarenne-Charpentier[1☯], Hassan El Btaouri[1☯]*

1 UMR-CNRS 7369 Matrice Extracellulaire et Dynamique Cellulaire (MEDyC), UFR SEN, URCA, Reims cedex, France, **2** Technical Platform for Cellular and Tissue Imaging (PICT), UFR Pharmacie, URCA, Reims, France

☯ These authors contributed equally to this work.
‡ AH and MM also contributed equally to this work.
* hassan.elbtaouri@univ-reims.fr

Abstract

Multidrug resistance (MDR) is a major obstacle to successful cancer chemotherapy. A typical form of MDR is due to the overexpression of membrane transport proteins., such as Glycoprotein-P (P-gp), resulting in an increased drug efflux preventing drug cytotoxicity. P-gp is mainly localized on the plasma membrane; however, it can also be endocytosed resulting in the trafficking of P-gp in endoplasmic reticulum, Golgi, endosomes, and lysosomes. The lysosomal P-gp has been found to be capable of transporting and sequestering P-gp substrates (e.g., Doxorubicin (Dox)) into lysosomes to protect cells against cytotoxic drugs. Many translational studies have shown that low-density lipoprotein receptor-related protein-1 (LRP-1) is involved in endocytosis and regulation of signalling pathways. LRP-1 mediates the endocytosis of a diverse set of extracellular ligands that play important roles in tumor progression. Here, we investigated the involvement of LRP-1 in P-gp expression and subcellular redistribution from the cell surface to the lysosomal membrane by endocytosis and its potential implication in P-gp-mediated multidrug resistance in MCF-7 cells. Our results showed that MCF-7 resistant cells (MCF-7R) overexpressed the P-gp, LRP-1 and LAMP-1 and were 11.66-fold resistant to Dox. Our study also revealed that in MCF-7R cells, lysosomes were predominantly high density compared to sensitized cells and P-gp was localized in the plasma membrane and lysosomes. LRP-1 blockade reduced lysosomes density and level of LAMP-1 and P-gp. It also affected the subcellular distribution of P-gp. Under these conditions, we restored Dox nuclear uptake and ERK 1/2 activation thus leading to MCF-7R cell sensitization to Dox. Our data suggest that LRP-1 is able to modulate the P-gp expression and subcellular redistribution by endocytosis and to potentiate the P-gp-acquired Dox resistance.

1. Introduction

Drug resistance is an obstacle that impairs the success of cancer therapies. This resistance occurs after repeated cycles of chemotherapy leading to the acquisition of tumor resistance [1]. Multiple mechanisms contribute to drug resistance, such as increased drug efflux, altered drug metabolism and activation of downstream transduction pathways [2, 3]. Recent studies have suggested that immune cells in tumor microenvironment (TME) play important roles in mediating acquired drug resistance [4, 5]. Indeed, reduced number of cytotoxic effector immune cells within the TME drive the tumor-mediated immunosuppression and could trigger acquired resistance development against immune checkpoint inhibitors [6–8]. Additionally, it has also been reported that the extracellular matrix influences tumor chemoresistance [9]. In fact, In fact, several studies confirmed the implication of collagen and fibronectin in chemoresistance induction [10–12]. Our previous study demonstrated that Thrombospondin-1 contribute to the modulation of P-gp drug resistance in thyroid carcinoma FTC-133 cells [13].

The main mechanism of cell drug resistance involves the ABC (ATP-binding cassette) protein transporters which pump drug molecules out of cells [14]. ABC transporters include the multidrug resistance (MDR) protein or P-glycoprotein (MDR1/P-gp/ABCB1), the multidrug resistance-associated proteins (MRP1, ABCC1) and the breast cancer resistance proteins (BCRP, ABCG2) [15, 16]. P-gp, a 170-kDa membrane protein, is localized not only at the plasma membrane but also in intracellular compartments such as endoplasmic reticulum and Golgi [17–19]. Several studies have suggested that P-gp, when present at the plasma membrane, functions as a pump to efflux drug out the cell, but also, when localised at the lysosomal membrane, can play another functional role inducing drug resistance. In this case, lysosomal membrane P-gp transports substrates into the organelle, thus preventing drugs effects. [20]. These results suggested that there was an intracellular pool of P-gp that originated from the plasma membrane by an endocytosis pathway. Several studies have focused on the function of P-gp and ways to overcome P-gp-mediated MDR [2, 14, 21, 22]. However, little is known about the processes of cellular distribution of P-gp and its intracellular traffic.

The LDL (low-density lipoprotein) receptor family is a group of transmembrane proteins that bind a variety of ligands. Currently identified LRP-1 ligands include proteases, protease inhibitor complexes, extracellular matrix proteins, growth factors, toxins, and viral proteins [23–26]. LRP-1 (LDL receptor-related protein 1) is an important member of this family with multiple ligand binding sites and is expressed in several cell types. [27–29]. LRP-1 is synthesized as a precursor glycoprotein of 600 kDa and cleaved into two non-covalently associated subunits (α, 515 kDa and β, an 85 kDa). The endocytosis and intracellular trafficking of LRP-1 plays a key role in regulating the cellular functions and activities of several receptors and plasma membrane proteins that molecularly interact with LRP-1, such as platelet-derived growth factor receptor β (PDGFR β), urokinase-plasminogen activator receptor (uPAR) and β1-integrin [30–33]. The broad ligands that bind LRP-1 enable this receptor to serve as a sensor of the cellular microenvironment and regulator of cell signalling and cell physiology in response to numerous extracellular stimuli [32, 34]. LRP-1 also regulates cell signalling by trafficking receptor-ligand complexes into endosomes and consequently by controlling the abundance of these receptors at the plasma membrane [35].

Previous work showed that LRP-1 promoted invasion, survival or metastatic dissemination of thyroid carcinoma [36] and breast cancer cells [37–39]. Other studies established that LRP-1 may constitute a strong predictive marker of clinical outcome in 12 types of cancers [40].

With the purpose of establishing a functional relationship between LRP-1-mediated endocytosis and P-gp acquired-resistance, here we explored the ability of LRP-1 to modulate P-gp-induced resistance to Dox in MCF-7 cells.

2. Materials and methods

2.1. Materials

MCF-7, a human breast carcinoma cell line derived from the pleural effusion metastasis, weas purchased from ATCC (USA). Dox was purchased from Farmitalia (Italy). MCF-7 resistant cells (MCF-7R) were obtained from MCF-7 parental cells by increased Dox treatment. DMEM/F-12, trypsin and Lipofectamine RNAiMAX were from Invitrogen (France). Bovine fetal serum was from Dutscher (France). LRP-1 polyclonal antibody '*ab92544*' was from Abcam (France). Caspase-7 '*#9492*', ERK 1/2 '*#4695*', Phospho-ERK 1/2 '*#4370*', LAMP-1 '*#9091*' and P-gp '*#13342*' antibodies were from Cell Signaling Technology (France). LRP-1 siRNA kit '*sc-40101*' was purchased from Santa Cruz Biotechnology (USA). Kit ECL was from Amersham (Germany). U0216, a elective inhibitor of MEK-1 and MEK-2, was from Cell Signaling Technology (France). UptiBlue and BCA kit '23225' were from Uptima (Thermofisher, France). CaspACE assay kit '*G8091*' was from Promega (France). β-actin antibody '*A5316*', invertase enzyme '*I9274*' and all other reagents were from Sigma (USA). Histidine-tagged RAP was purified as previously described [41] and used as an antagonist of LRP-1-dependent endocytosis [41, 42].

2.2. Cell culture

MCF-7R cells were selected from MCF-7 parental cells by gradual increase of the Dox concentration (from 10 to 800 nM) according to protocol of Chen et al. [43] modified. MCF-7 and MCF-7R cells were cultured in 75 cm^2 flasks at 37°C containing DMEM/F-12 (1:1) supplemented with 10% (v/v) foetal calf serum, streptomycin (100 μg/ml) and penicillin (100 IU/ml) in a 5% CO_2. Cells were then trypsined and cultured in appropriate well plates for cell viability, flow cytometry, spectrofluorometry, Western blot analysis, mRNA extraction and caspase assay.

2.3. Cell viability determination

Cells plated in 96-well plates at 10^4 cells/mL were incubated until they reached the exponential phase of growth. The medium was then substituted with serum free medium with or without different Dox concentrations (from 0 to 10 μM), in presence or absence of RAP (500 nM) or U0126 (1 μM). After 48 h and 72h incubation, 10% (v/v) UptiBlue was added, and the cells incubated for 3 additional hours. The viability was determined by spectrofluorometry (λex: 530–560 nm; λem: 590 nm). The results were calculated as percentage of control as follows: (% of treated viable cells versus untreated viable cells).

2.4. Nuclear incorporation of Dox

Cells plated in Petri dish at 10^4 cells/mL were incubated with Dox 1 μM in presence or absence of RAP (500 nM) for 5 hours and placed in the medium without phenol red. The nuclear Dox incorporation was measured by spectrofluorometry over the wavelength range 500–700 nm [44]. The nuclear Dox was semi-quantified by the fluorescence emission intensity of the band at 690 nm (within the nuclear perimeter of 50 nuclei) optical fields. The data of 5 different random was analysed by Labspec software (Horiba).

2.5. Western blot

Cells were centrifuged at 3000 g for 5 min (4°C) and washed with ice-cold PBS. Cell pellets were lysed by lysis buffer containing 10 mM Tris pH 7.4 (150 mM NaCl, 5 mM EDTA, 1 mM orthovanadate, 1 mM dithiothreitol, 10 μg/mL leupeptin, 10 μg/mL aprotinin, 10% (v/v)

glycerol, 1% (v/v) Brij). Cell lysates were placed on ice for 20 min and centrifuged (14,000 g, 15 min, 4˚C). The protein concentration was determined by BCA assay kit following the manufacturer's instructions of Thermofisher scientific '*2161296*'. Proteins were separated using SDS-PAGE analytical technique according to the Bio-rad PROTEAN specification. In brief, 20–25 μg of protein sample were mixed with 4X sample loading buffer and heated at 70˚C for 10 min. Samples were then loaded on the gel (10% polyacrylamide). Electrophoresis was performed at room temperature for approximately 45 min using a constant voltage (200V) in 1X solution of SDS running buffer. The proteins were then transferred to nitrocellulose sheets for approximately 125V/60 min using the Trans-BlotⓇ Cell system according to the Bio-rad manufacturer's instructions. The nitrocellulose sheets were then probed with the appropriate antibodies (polyclonal anti-LRP-1: dilution 1/1000; polyclonal anti-caspase-7: dilution 1/1000; polyclonal anti-P-gp: dilution 1/1000; polyclonal anti-PhosphoERK1/2: dilution 1/1000; polyclonal anti-ERK1/2: dilution 1/1000; polyclonal anti-LAMP-1: dilution 1/1000; monoclonal anti-β-actin: dilution 1/8000). Horseradish peroxidase-conjugated IgG were used as secondary antibodies (dilution 1/4000 and 1/10,000 respectively) and the detection was realised by enhanced chemiluminescence kit.

2.6. Caspase-3/7 activity

Cells were washed twice with PBS and scrapped with ice-cold lysis buffer. Caspase-3/7 activity was measured by incubating 50 μg of cytosolic fraction with a colorimetric substrate and absorbance was measured at 405 nm according to the Promega manufacturer's instructions 'TB323'.

2.7. Cell transfection

Cell transfection was realized using Lipofectamine RNAiMAX following the manufacturer's instructions of Invitrogen 'MAN0007825 Rev. 1.0. Briefly, MCF-7 cells were incubated for 1–3 days at 37˚C with either non-targeting control scRNA (scRNA-MCF-7R cells) or siRNA specific to LRP-1 (siRNA- MCF-7R cells) and Lipofectamine RNAiMAX Reagent (1:1 ratio).

2.8. Immunofluorescence and internal vesicles labelling

MCF-7R cells, scRNA-MCF-7R cells and siRNA-MCF-7R cells were plated onto 1% gelatin-coated glass slides for 24 h at 37˚C. MCF-7R cells were then incubated in presence or absence of RAP (500 nM) for 12h. Cells were fixed in phosphate buffered saline (PBS) containing 4% paraformaldehyde for 15 min at room temperature and incubated for 1 h in PBS containing 1% bovine serum albumin and overnight at 4˚C with primary antibodies raised against LRP-1 (1/500) or LAMP-1 (1/600). Then, the slides were washed five times with ice-cold PBS and incubated with secondary antibodies conjugated to Alexa Fluor 488 (1/500) or Alexa Fluor 568 (1/500) for 2 h at room temperature. Confocal microscopy images of fixed cells were collected with a Zeiss (Oberkochen, Germany) LSM710 Meta confocal microscope using either a ×63 Plan Apochromat objective (oil immersion, 1.40 NA, DIC) at a 132 nm.pixel-1 resolution, leading to a slight XY oversampling. The Zen software program was used to acquire images as previously detailed in [41].

2.9. Isolation of endocytic organelles by density gradient centrifugation

Following incubation in presence or absence of RAP (500 nM) for 12h, 2.10^6 cells were washed three times with ice-cold PBS and suspended in homogenization buffer for isolation of endocytic organelles using a gradient centrifugation as described by de Araujo et al. (2015) [45].

After centrifugation, aliquots (1 ml) were collected and the sucrose gradient was analysed using invertase enzyme assay as described by Gusakov et al (2011) [46]. Aliquots were conserved at -80°C.

2.10. Sucrose assay

Sucrose in aliquot was measured using DNS Assay as described by Gusakov et al (2011) [46]. Briefly, 50 μL of each diluted aliquot (10x) was incubated with 100 μl of acetate buffer (pH 4.7) and 50 μL of invertase enzyme (100 unit.mL^{-1}) for 60 min at 37°C. Then, the DNS reagent (100 μL) was added, and the mixture was incubated in a boiling water bath for 5 min. After cooling to room temperature, the absorbance of the supernatant at 540 nm was measured.

2.11. Statistics

Each experiment was realized at least in triplicate with three independent cultured cells. Data were presented as mean ± SEM. The statistical calculation was based on the Student's t-test. p values referring to corresponding control are ** and ¥¥ $p < 0.01$, *** and ¥¥¥ $p < 0.001$, **** and ¥¥¥¥ $p < 0.0001$.
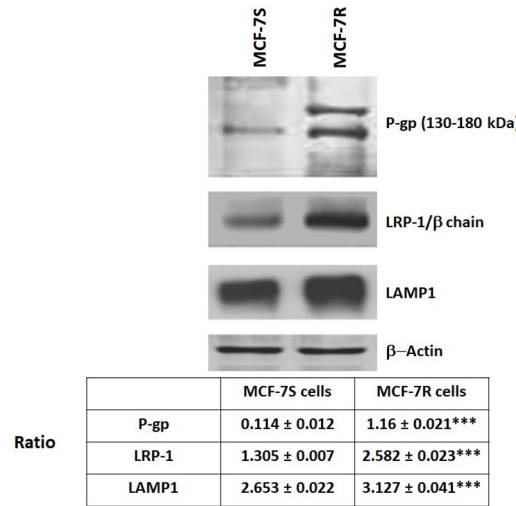
3. Results

To study LRP-1 effects on multidrug resistant cells, two human breast carcinoma cells were used: parental MCF-7 cells sensitive to Dox called MCF-7S and MCF-7 cells resistant to Dox that were obtained by stepwise exposure of MCF-7S cells to increasing doses of Dox and called MCF-7R [47]. No significant difference in the morphology and growth rates between the two-line cells MCF-7S and MCF-7R cells was observed.

We first analysed the expression of P-gp and LRP-1 in both cell types and Western blot analysis clearly showed a higher level of P-gp and LRP-1 expression in MCF-7R cells compared to MCF-7S cells (Fig 1).

The MCF-7R cell chemosensitivity to Dox was compared to that of MCF-7S cells by cell incubation with increasing Dox concentrations with or without 500 nM RAP, a universal antagonist of ligand binding to LRP-1 (Fig 2). As expected, Dox decreased MCF-7S cell viability in a dose-dependent manner with an IC$_{50}$ = 0.5 and 0.3 μM for a period of 48 and 72h respectively (Fig 2A). In contrast, MCF-7R cells exhibited a lower sensitivity to Dox, confirmed by an increase of IC$_{50}$ to 3.8 and 3.5 μM for a period of 48 and 72h respectively and an increase of RI (resistance index = ratio IC$_{50}$ MCF-7R/IC$_{50}$ MCF-7S) to 7.6 and 11.66 for a period of 48 and 72h respectively (Fig 2B and 2D). The P-gp mediated Dox resistance was confirmed by Verapamil (P-gp inhibitor), indeed, Verapamil (5 μM) pre-treatement of MCF-7R cells sensitized cells to Dox cytotoxic effects (Fig 2C). Moreover, treatment of MCF-7R cells with RAP induced an increase of Dox cytotoxicity confirmed by lower IC$_{50}$ (1.4 and 1.5 μM for a period of 48 and 72h respectively) and RI (Fig 2D). These results clearly demonstrated that RAP partially restored the MCF-7R cell sensitivity to Dox.

To clarify the role of LRP-1 in cell resistance, LRP-1 expression was silenced by small RNA interference in MCF-7R cells (called siRNA-MCF-7R cells). The efficiency of the transfection was evaluated in MCF-7R cells transfected with scrambled RNA (called scRNA-MCF-7R cells). As shown in Fig 3A, Western blot analysis revealed a decrease of the LRP-1 and P-gp expression in siRNA-MCF-7R cell as compared to that in scRNA-MCF-7R cells.

The chemo-sensitivity of these cells was then evaluated in presence of increasing Dox concentrations at 48 and 72 hours (Fig 3B). The cell viability assays clearly showed that Dox induced a significant decrease of siRNA-MCF7R cell viability and reduced the value of IC$_{50}$ from 4.2 to 1μM and from 2.8 to 0.5μM for a period of 48 and 72 hours respectively (Fig 3C).

	MCF-7S cells	MCF-7R cells
P-gp	0.114 ± 0.012	1.16 ± 0.021***
LRP-1	1.305 ± 0.007	2.582 ± 0.023***
LAMP1	2.653 ± 0.022	3.127 ± 0.041***

(Row label: **Ratio**)

Fig 1. Overexpression of P-gp and LRP-1 in MCF-7R. MCF-7S and MCF-7R cells were cultured for 24 hours. Detection of P-gp, Lamp-1 and LRP-1/β chain was evaluated by Western-blot. β-actin antibody was used as a control. The results were represented by three independent experiments. Quantity one software was used to quantify the intensity of the bands. Student's t-test was used for the statistical significance of different values. *** p<0.001 for MCF-7R cells compared to MCF-7S cells. The ratio was calculated with densitometry value of the protein of interest/ densitometry value of the β-actin.

https://doi.org/10.1371/journal.pone.0285834.g001

C

MCF-7R cell viability (% versus control)		
	Dox 1 µM	Dox 1 µM + Verapamil
48h	72 ± 5.2	38 ± 6.6****
72h	68 ± 3.6	25 ± 4.7****

D

		MCF-7S		MCF-7R	
		-RAP	+RAP	-RAP	+RAP
48h	IC₅₀ (µM)	0.5	0.4	3.8	1.4***
	RI			7,6	3,5***
72h	IC₅₀ (µM)	0.3	0.25	3.5	1.5***
	RI			11.66	6***
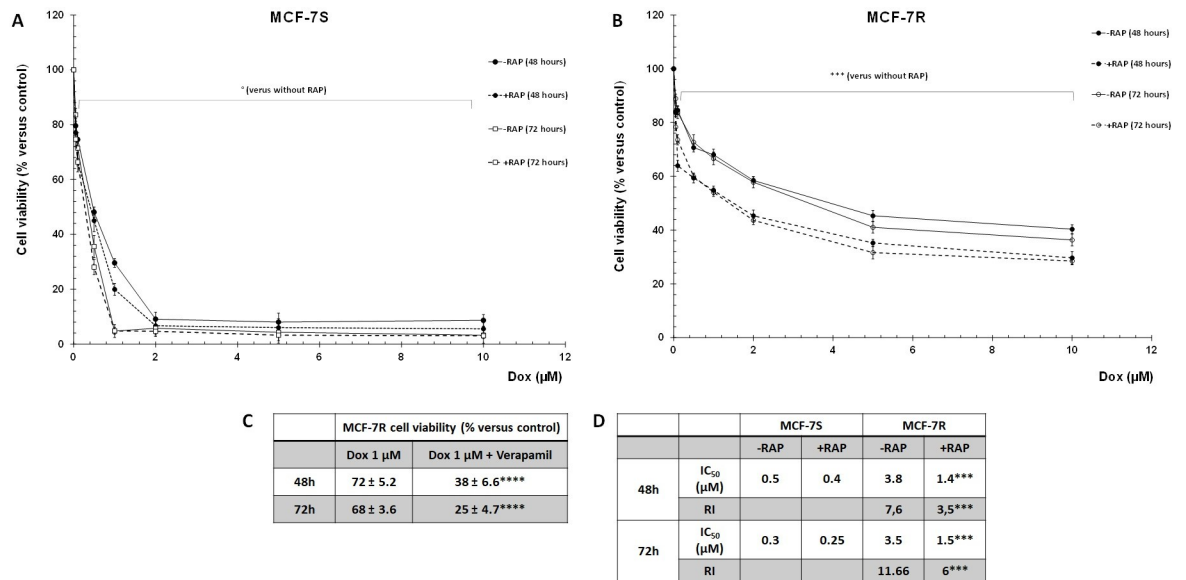
Fig 2. RAP sensitized MCF-7R cells to Dox cytotoxic effects and reduced IC$_{50}$. A and B, MCF-7S and MCF-7R cells were treated with different Dox concentrations (from 0 to 10 µM) with or without 500 nM RAP. After 48 and 72h, cell viability was measured by UptiBlue Viable Cell Counting Assay. The results were presented as percentage of control and represented with standard deviation (S.D.) of at least three independent experiments. Student's t-test was used for the statistical significance of different values.° NS, *** p<0.001 compared to cells cultured without RAP. **C**, MCF-7R cells were pretreated with Verapamil (5 µM) for 6h and incubated with Dox (1 µM). After 48 and 72h, cell viability was measured using UptiBlue Viable Cell Assay. The results obtained from three independent experiments (% of control) were represented with standard deviation (S.D.). Student's t-test was used for the statistical significance of different values. **** p<0.0001 for Verapamil and Dox-MCF-7R cells compared to Dox-MCF-7R cells. **D**, summary table of IC$_{50}$ and RI (resistance Index). IC$_{50}$ represents the mean half maximal inhibitory concentration. RI was assessed using the quotient of the IC$_{50}$ values (IC$_{50}$ MCF-7R/IC$_{50}$ MCF-7) in each treatment conditions. Student's t-test was used for the statistical significance of different values. *** p<0.001 for RAP-MCF-7R cells compared to untreated MCF-7R cells.

https://doi.org/10.1371/journal.pone.0285834.g002
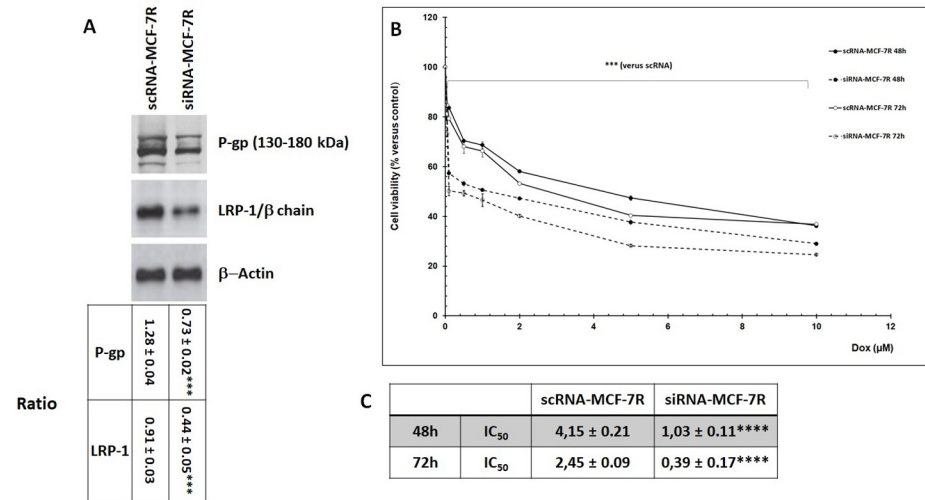
Fig 3. LRP-1 silencing by siRNA reduced P-gp expression and sensitized MCF-7R cells to Dox. A, scRNA-MCF-7R and siRNA-MCF-7R cells were cultured for 24 hours. Detection of P-gp and LRP-1/β chain was evaluated by Western-blot. β-actin antibody was used as a control. The intensity of the bands was quantified by densitometry using quantity one program. Student's t-test was used for the statistical significance of different values. *** p<0.001 for siRNA-MCF-7R cells compared to scRNA-MCF-7R cells. The ratio was calculated with densitometry value of the protein of interest/densitometry value of the β-actin. **B**, scRNA-MCF-7 and siRNA-MCF-7R cells were incubated with Dox at concentrations ranging from 0 to 10 μM. After 48 and 72h, cell viability was measured using UptiBlue Viable Cell Assay. The results obtained from three independent experiments (% of control) were represented with standard deviation (S.D.). Student's t-test was used for the statistical significance of different values. *** p<0.001 for siRNA-MCF-7R cells compared to scRNA-MCF-7R cells. **C**, summary table of IC$_{50}$. IC$_{50}$ represents the mean half maximal inhibitory concentration. Student's t-test was used for the statistical significance of different values. **** p<0.0001 for siRNA-MCF-7R cells compared to scRNA-MCF-7R cells.

These results demonstrated that LRP-1 silencing sensitized MCF-7 resistant cells to Dox and confirm the role of LRP-1 in MCF-7 cell chemoresistance.

As previously reported by Rath et al. [48], Dox decreased cell viability by triggering apoptosis in a caspase-dependent manner. However, MCF-7 cells do not express caspase-3, and caspase-7 might compensate for this lack of expression [49]. We thus analysed caspase-7 activation in MCF-7S and MCF-7R cells incubated with or without Dox (1 μM) in presence or in absence of RAP (500 nM) for 12 h. The caspase-7 activity was measured by Western-blot and Caspase-Glo 3/7 assay System (Fig 4). We showed that Dox induced the caspase-7 activation in MCF-7S cells and the presence of RAP amplified this effect. In MCF-7R cells, Dox alone induced a very low activation of caspase-7 compared to MCF-7S cells. However, RAP addition amplified the Dox-induced activation of the caspase-7. This suggests that LRP-1 could be responsible for the low level of caspase-7 activation and the decrease of Dox cytotoxic effect. We then analysed caspase-7 activation in transfected cells and our data showed that both caspase-7 cleavage and activity was significantly increased in siRNA-MCF-7R cells thus confirming that LRP-1 was involved in MCF-7 cell resistance to Dox apoptosis effects (Fig 4).

Since the cytotoxic effect of dox is related to its nuclear concentration. we then measured nuclear Dox level in both parental and resistant cells. Fig 5 showed that nuclear Dox level was about 3 times weaker in MCF-7R cells than in MCF-7S cells. The MCF-7R cell pre-treatment by Verapamil (5 μM) increased Dox nuclear uptake about 2.2 times compared MCF-7R treated only by Dox. This result established the P-gp implication in MCF-7R resistance to Dox by decreasing its subcellular accumulation. RAP significantly increased drug nuclear accumulation in MCF-7S as well as in MCF-7R cells and demonstrated that RAP reduced P-gp-induced efflux Dox out of the cell. Moreover, LRP-1 silencing increased drug nuclear accumulation,
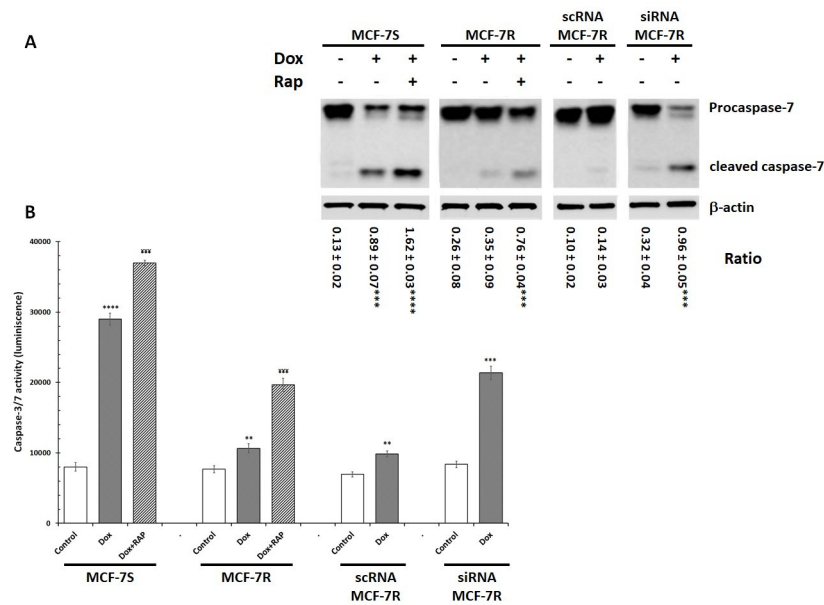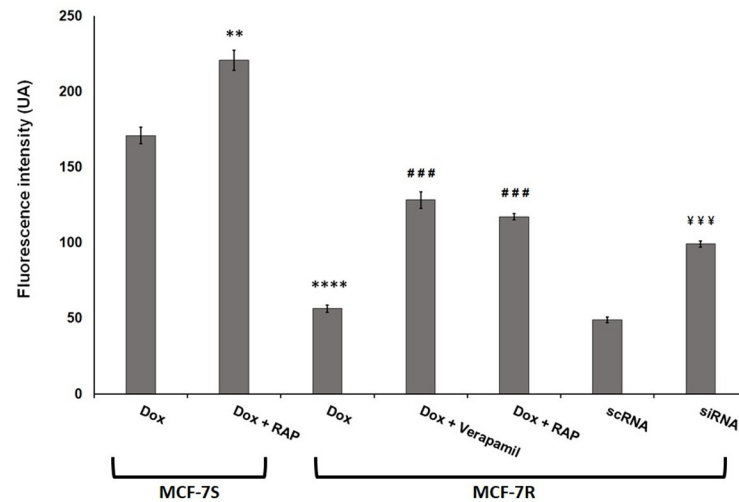
Fig 4. RAP and LRP-1 silencing by siRNA promoted the caspase-7 activation in Dox-treated MCF-7R cells. MCF-7S, MCF-7R, scRNA-MCF-7R and siRNA-MCF-7R cells were incubated with 5 μM Dox with or without 500 nM RAP for 12 hours. A, Procaspase-7 and cleaved caspase-7 were detected by Western blotting. β-actin antibody was used as a control. The results were represented by three independent experiments. Quantity one software was used to quantify the intensity of the bands. Student's t-test was used for the statistical significance of different values. *** p<0.001 and **** p<0.0001 for treated cells compared to untreated cells. The ratio was calculated with densitometry value of the protein of interest/ densitometry value of the β-actin. **B**, Caspase-7 activity was measured by caspACE assay kit. The results obtained from three independent experiments were represented with standard deviation (S.D.). Student's t-test was used for the statistical significance of different values. ** p<0.01 and **** p<0.0001 compared to control cells. ¥¥¥ p<0.001 compared to Dox-treated cells.

thus confirming that LRP-1 could modulate P-gp-acquired resistance. We therefore investigated the interrelation between the LRP-1 level and the expression and localization of P-gp in MCF-7S and MCF-7R cells. Thus we analysed LRP-1 and P-gp expression in MCF-7S and MCF-7R cells incubated with or without Dox (1 μM) in presence or in absence of RAP (500 nM). Western blot analysis showed a LRP-1 expression higher in MCF-7R cells than in MCF-7S cells, and its level decreasing with incubation period. Dox had no effects on LRP-1 expression (Fig 6A). The P-gp expression analysis showed that P-gp level was not affected by Dox treatment. However, addition of 500 nM RAP significantly reduced the P-gp expression in MCF-7R cells (Fig 6B). These results confirmed that LRP-1 could modulate the P-gp expression in MCF-7R cells.

P-gp is localized in many intracellular organelles, including endoplasmic reticulum (ER), endosome, lysosome and proteasome [17–19, 50–52]. Furthermore, the endosomal localization is involved in trafficking/recycling P-gp between the cellular pool and the plasma membrane [19]. We thus hypothesised that decreased P-gp expression induced by RAP could result in a decrease of this transporter in the lysosomal compartment. Therefore, we analysed the intracellular localization of P-gp in presence or absence of RAP in MCF-7R cells by confocal immunofluorescence microscopy using anti-LAMP-1 antibody as a lysosome marker (Fig 7). Merged image of P-gp (red) and LAMP-1 (green) revealed distribution of P-gp within lysosome (gold). LRP-1 blockade using RAP reduced P-gp expression and its distribution in lysosomes. This effect was also observed by a siRNA strategy against LRP-1 showing a decrease in P-gp expression and distribution in lysosomes. In these siRNA-MCF-7R cells, we also

Fig 5. RAP and LRP-1 silencing by siRNA increased Dox nuclear uptake in MCF-7R cells. MCF-7S, MCF-7R, scRNA-MCF-7R and siRNA-MCF-7R cells were placed in petri dishes, pretreated with Verapamil (1 µM) for 6h and with 4 µM Dox with or without 500 nM RAP for 5h. The cells were washed with PBS free of drugs at 4°C. The nuclear Dox was followed through its fluorescence emission spectra by confocal laser microspectrofluorometry. A nuclear spectrum of treated cells was obtained over the wavelength range 500–700 nm [44]. The semi-quantification of nuclear Dox incorporation was evaluated by the fluorescence emission intensity of the band at 590 nm. The results represent mean ± standard deviation (S.D.) of at least three independent experiments. The data was analysed by Labspec software (Horiba). Student's t-test was used for the statistical significance of different values. **** $p < 0.0001$ versus Dox-treated MCF-7S cells, ### $p < 0.001$ versus Dox-treated MCF-7R cells and ¥¥¥ $p < 0.001$ compared to scRNA-cells.

observed a reduction in the intensity of the fluorescent signal corresponding to the LAMP-1. This result confirmed that LRP-1 affected the localization of P-gp in lysosome and altered lysosomal Dox trapping.

To confirm these results, we used density gradient centrifugation to separate intracellular components in particular endocytic organelle. Cell lysate was subjected to sucrose-gradient centrifugation in order to separate the lysososomal fractions from the soluble proteins and disrupted membranes. After centrifugation, we measured sucrose percentage in collected consecutive fractions. The result confirmed that sucrose gradient was maintained between 12 and 62%. Then, we analysed lysosomes and P-gp expression in all collected fractions by Western blot using anti-LAMP-1 and anti-P-gp antibodies respectively (Fig 8). In MCF-7S cells, the fractions 22–44% (of sucrose) contained lysosomes with the majority being concentrated in fraction 30% (Fig 8A). In MCF-7R cells, lysosomes were mainly localized in the fractions 24–51% (of sucrose) with a significant level in the fractions 35–38% of sucrose. This suggested that lysosomes have high density in MCF-7R cells. P-gp detection by Western-blot showed that P-gp displayed a continuous distribution in fractions 17–51% sucrose, peaking in fractions 30–44% corresponding to lysosomal localization (Fig 8B). LRP-1 blockade using RAP or SiRNA specific to LRP-1 significantly decreased the level and density of lysosome in MCF-7R cells. Indeed, LAMP-1 expression was reduced and was essentially localized in the fractions 24–35% (of sucrose) in RAP-treated cells and siRNA-MCF-7R cells. The distribution profile of lysosomes overlapped with that obtained in MCF-7S cells (Fig 8E). We also analysed the LAMP-1 level in all fractions. The results showed that LAMP-1 expression is very high in MCF-7R cells compared to MCF-7S cells. RAP or siRNA treatment of cells reduced the LAMP-1 level in MCF-7R cells (Fig 8G). P-gp expression was also decreased in fractions containing lysosomes
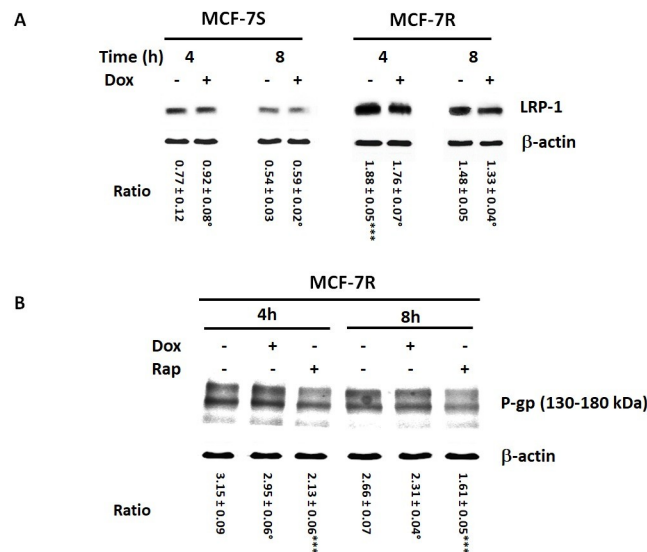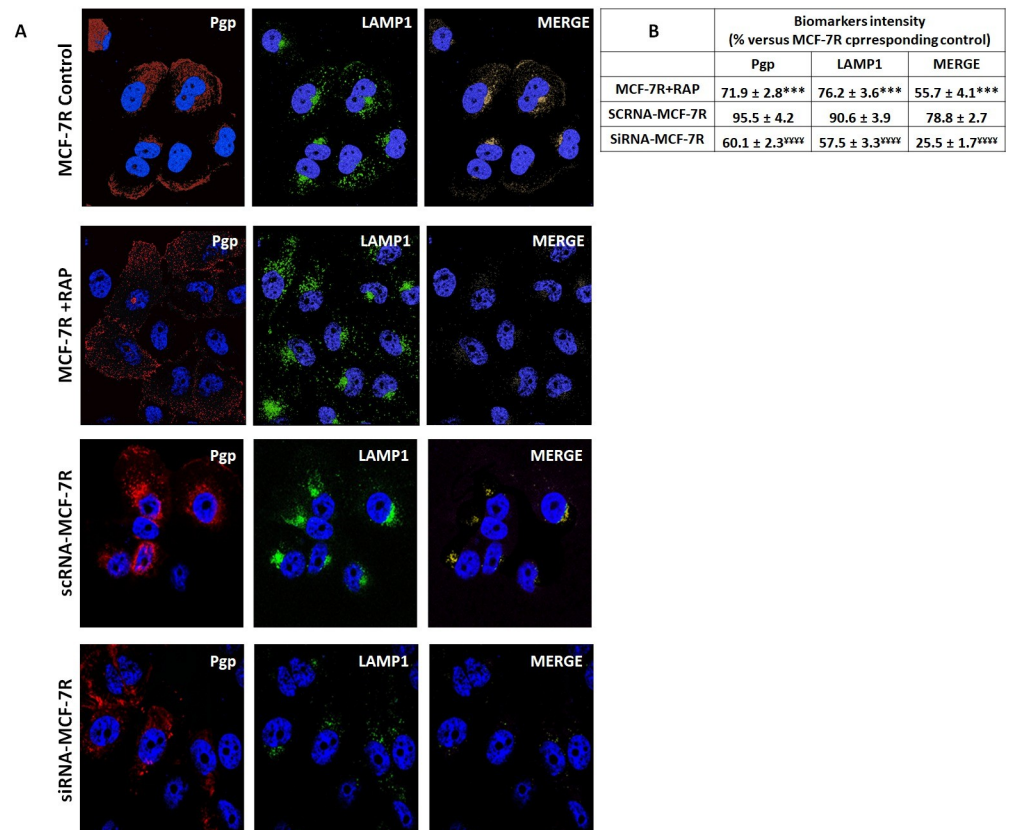
Fig 6. RAP reduced the P-gp expression in MCF-7R cells. A, MCF-7S and MCF-7R cells were incubated with or without 5 μM Dox for 4 and 8 hours. Detection of LRP-1/β chain was evaluated by Western-blot. β-actin antibody was used as a control. A representative blot of three independent experiments was shown. The intensity of the bands was quantified by densitometry using quantity one program. Student's t-test was used for the statistical significance of different values. *** p < 0.001 for MCF-7R versus MCF-7S cells,˚ NS for Dox-treated cells versus untreated cells. **B,** MCF-7R cells were incubated with or without 500 nM RAP for 4 and 8 hours. Detection of P-gp was evaluated by Western-blot. β-actin antibody was used as a control. A representative blot of three independent experiments was shown. The intensity of the bands was quantified by densitometry using quantity one program. Student's t-test was used for the statistical significance of different values. *** p < 0.001 for RAP-treated cells versus MCF-7S cells,˚ NS for Dox-treated cells versus untreated cells. The ratio was calculated with densitometry value of the protein of interest/ densitometry value of the β-actin.

https://doi.org/10.1371/journal.pone.0285834.g006

after RAP treatment MCF-7R cells. Similar results were obtained in siRNA-MCF-7R cells (Fig 8C and 8D and 8F and 8G).

Next, we investigated the signalling pathways involved in cell apoptosis induced by Dox and modulated by LRP-1. Several studies have shown that the p38 MAPK and PI3K/Akt pathways apparently exert a regulatory effect with regard to the induction of cell death; the sustained activation of ERK1/2 appears to be positively related to apoptosis induced by anticancer DNA-damaging drugs in several cell lines [53]. Therefore, we analysed the effects of Dox on p38 and ERK1/2 MAPKs activation in both MCF-7S and MCF7-R cells. The cells were incubated in presence or absence of Dox (1 μM) with or without RAP (500 nM) for 0.5, 1 and 2 hours and phosphorylation of ERK1/2, p38 and AKT was analysed by Western-blot (Fig 9). Results showed that Dox treatment modulated ERK1/2 phosphorylation but had no effect on p38 and AKT (Fig 9A). Indeed, Dox induced ERK1/2 phosphorylation in MCF-7S with a maximum at 1h of time incubation (Fig 9B). This effect was amplified by RAP treatment while RAP alone has no effect on EKR1/2 expression and basal activity (Fig 9C). In MCF7R cells, Dox induced ERK1/2 phosphorylation in the presence of RAP whereas alone had no effect on this MAPK. This result showed that P-gp expression was correlated with a decrease of ERK1/2 phosphorylation and suggested that P-gp-expressed in MCF-7R inhibited the ERK1/2 phosphorylation by Dox. However, RAP treatment restored the Dox-induced ERK1/2 activation.

To determine a possible relationship between ERK1/2 phosphorylation and MCF-7 cell apoptosis, we treated cells with U-0126, a cell permeable ERK1/2 signalling pathway inhibitor and analysed cell viability. As shown in Fig 10, U-0126 prevented Dox-induced apoptosis in

B	Biomarkers intensity (% versus MCF-7R cprresponding control)		
	Pgp	LAMP1	MERGE
MCF-7R+RAP	71.9 ± 2.8***	76.2 ± 3.6***	55.7 ± 4.1***
SCRNA-MCF-7R	95.5 ± 4.2	90.6 ± 3.9	78.8 ± 2.7
SiRNA-MCF-7R	60.1 ± 2.3¥¥¥¥	57.5 ± 3.3¥¥¥¥	25.5 ± 1.7¥¥¥¥

Fig 7. RAP and LRP-1 silencing by siRNA reduced P-gp expression and its distribution in lysosomes of MCF-7R cells. A, MCF-7R cells were seeded onto 1% gelatin-coated glass slides for 12 h at 37˚C with or without 5 μM Dox in presence or absence of 500 nM RAP for 12 hours. P-gp and Lamp-1 staining respectively with Alexa Fluor 467 and Alexa Fluor 488 were carried out before confocal microscopy analysis as shown in material and methods. The Zen software program was used to acquire images. Isosurface representations were realized using the AMIRA software program. **B,** The biomarker intensity was measured using ImageJ software. For each image, the signal intensity was measured at each cell. The value obtained was the average of the measurements. The results obtained from three independent experiments were represented with standard deviation (S.D.). Student's t-test was used for the statistical significance of different values. *** $p < 0.001$ compared to MCF-7R control cells. ¥¥¥¥ $p < 0.0001$ compared to scRNA-MCF-7R cells.

https://doi.org/10.1371/journal.pone.0285834.g007

MCF-7 cells and inhibited RAP-sensitized cell to Dox treatment. Collectively, our data support the hypothesis that ERK1/2 activation is essential for Dox mediated effects in MCF-7 cells.

4. Discussion

Multidrug-resistance (MDR) is a major obstacle to successful cancer chemotherapy and one important mechanism of MDR involves the plasma membrane glycoprotein P-gp. This transporter confers to cancer cells the ability to resist to cytotoxic drugs by pumping the drug out of the cells and thus reducing its cytotoxicity [21, 54, 55]. Several studies have demonstrated a negative correlation between P-gp expression levels and chemosensitivity in a range of human malignancies [55–57]. It is well established that P-gp actively effluxes cytotoxic substrates such as Dox [22]. Many studies showed that P-gp may traffic in cells through an intracellular endosomal system with protein vesicles transported to endosome compartments and thus forming an intracellular pool [51]. Indeed, P-gp has been reported to bound to the lysosomal membrane thus promoting the accumulation of the chemotherapeutic agent in acidic organelles
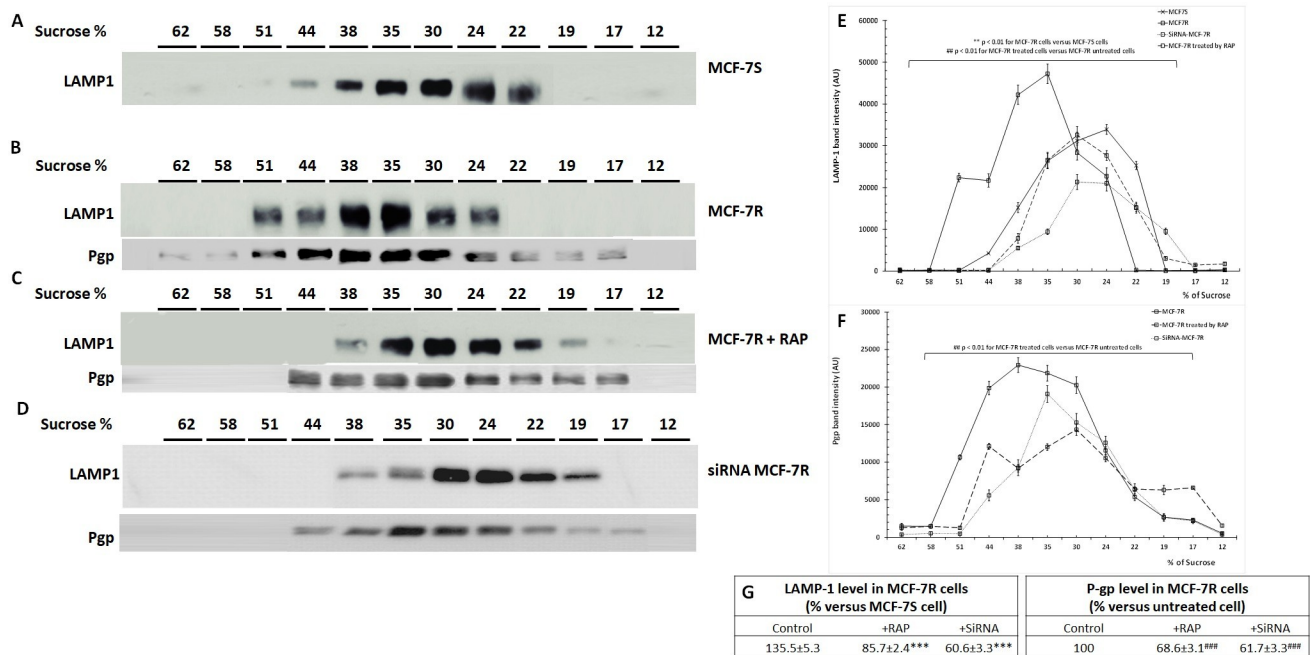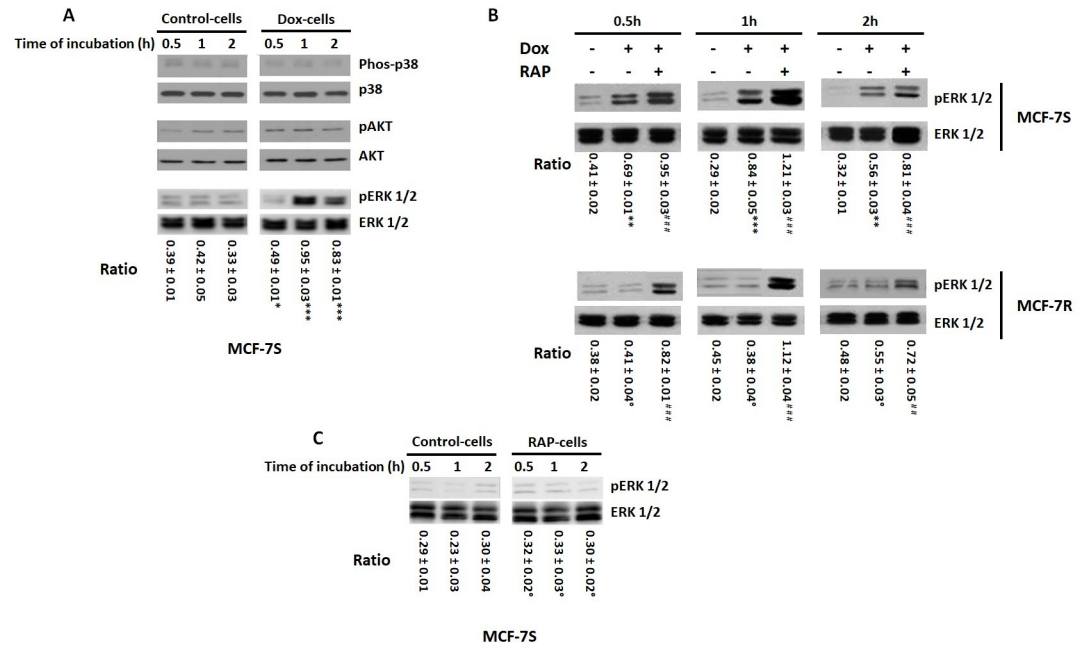
Fig 8. RAP and LRP-1 silencing by siRNA decreased the level and density of lysosome in MCF-7R cells. MCF-7S, MCF-7R cells that incubated with or without 500 nM RAP for 12 hours were used in this experiment. The endocytic organelles were isolated by density gradient centrifugation as detailed in Materials and Methods. sucrose gradient was analysed using invertase enzyme assay as described in Materials and Methods. Detection of P-gp and Lamp-1 were evaluated by Western-blot in all collected aliquots (A-D). The intensity of the bands was quantified by densitometry using quantity one program. Student's t-test was used for the statistical significance of different values. ** $p < 0.01$, *** $p < 0.001$ for MCF-7R cells versus MCF-7S cells, ## $p < 0.01$, ### $p < 0.001$ for MCF-7R treated cells versus MCF-7R untreated cells (E,F,G).

[58]. This strongly suggested the existence of both spatial and temporal distribution of P-gp and an intracellular traffic between the plasma membrane and endocytic organelles. Our study revealed that P-gp was localized both in and out late endosomes in MCF-7 human breast cancer cells. The localization of P-gp in endosomes has been suggested to serve as an intra-cellular reservoir to P-gp moving to the plasma membrane [17–19] and P-gp was internalized into cells from the plasma membrane to lysosomes via the endocytic pathway [59]. However, the detailed mechanisms of this P-gp intracellular traffic remain unclear.

LRP-1 is a large multi-functional receptor that regulates endocytosis of numerous ligands and transduces several signaling pathways. LRP-1 is detected in most tissues and highly expressed in liver, brain and lung [60]. In our study, we showed that the MCF-7 human breast cancer cells resistant to Dox expressed a high level of LRP-1 as compared to that of parental non-resistant cells. A higher LRP-1 expression has also been reported in MDA-MB-231 breast cancer cells and HCT-15 colorectal cancer cells [59] and can be related to the pro-tumoral effect of LRP-1 in some types of cancer cells. Concurrently, we observed that MCF-7R cells contained high density lysosomes compared to sensitive cells. LRP-1 has been shown to be essential for the recruitment of molecular adapters and signaling proteins for the initiation of endocytosis [61]. Thus, in our study, we observed an increase of lysosomes characterized by an elevated LAMP-1 level in MCF-7R cells. This result agreed with Dehay et al. studies (2010) showing a decrease of LAMP-1 level corresponded to a reduction of lysosomes number [62]. LAMP-1 was a major constituent of the lysosomal membrane and contributed to protection of the lysosomal membrane and its proteins from the hostile constituents such as hydrogen ion and proteases [63]. Indeed, downregulation of LAMP-1 has been previously shown to sensitize cells to lysosomal mediated death pathways [64] while increased levels of LAMP-1 mRNAs

Fig 9. RAP and LRP-1 silencing by siRNA promoted the ERK1/2 phosphorylation in Dox-treated MCF-7R cells. A, MCF-7S cells were incubated with 1 µM Dox for 0.5, 1 and 2 hours. Detection of pERK, ERK, pAKT, AKT, Phospho-p38 and p-38 were evaluated by Western-blot. A representative blot of three independent experiments was shown. The intensity of the bands was quantified by densitometry using quantity one program. The ratio was calculated with densitometry value of the pERK/ densitometry value of ERK. Student's t-test was used for the statistical significance of different values. *** p < 0.001, ** p < 0.01 for Dox treated cells versus untreated cells. **B**, MCF-7S and MCF-7R cells were incubated with 1 µM Dox with or without 500 nM RAP for 0.5, 1 and 2 hours. Detection of pERK and ERK were evaluated by Western-blot. A representative blot of three independent experiments was shown. The intensity of the bands was quantified by densitometry using quantity one program. The ratio was calculated with densitometry value of the pERK/ densitometry value of ERK. Student's t-test was used for the statistical significance of different values.˚ NS, ** p < 0.01 and *** p<0.001 for MCF-7 treated cells versus MCF-7S untreated cells, ## p < 0.01 and ### p < 0.001 versus Dox-treated cells. **C**, MCF-7S cells were incubated with or without 500 nM RAP for 0.5, 1 and 2 hours. Detection of pERK and ERK were evaluated by Western-blot. A representative blot of three independent experiments was shown. The intensity of the bands was quantified by densitometry using quantity one program. The ratio was calculated with densitometry value of the pERK/ densitometry value of ERK. Student's t-test was used for the statistical significance of different values.˚ NS, RAP treated cells versus untreated cells.

was observed in various human cancers [65–67]. This finding suggested a possible contribution of lysosomes in MCF-7R cell chemoresistance. LRP-1 blockade either by masking ligand binding sites with RAP or by silencing its expression by siRNA interference, reduced the density lysosomes and LAMP-1 level in MCF-7-R cells and sensitized them to Dox treatment. This hypothesis was supported by studies showing implicated lysosomes in drug resistance phenotypes and LAMP-1 in cancer metastasis [66, 68–70]. Several approaches have recently been developed to overcome drug resistance, including reduction of lysosome density by photo-destruction and by permeabilization of the lysosomal membrane or downregulation of LAMP-1 [66, 71].

In parallel, we showed that MCF-7R cells also overexpressed P-gp with a high level in lysosomes, suggesting that LRP-1 might lead to internalization of P-gp through an endocytic pathway. Indeed, LRP-1 blockade or silencing by siRNA reduced both P-gp expression and distribution in MCF-7R cells thus leading to increase Dox nuclear accumulation and therefore cell sensitization to Dox. lysosomal P-gp reduction did not lead to an elevation of its level in other cellular compartments such as the plasma membrane. Indeed, we showed a decrease in the global level of P-gp and also of LAMP-1. Several studies showed that LAMP-1 may protect lysosomal membrane proteins from degradation by proteases and hydrolases [72–75]. In our
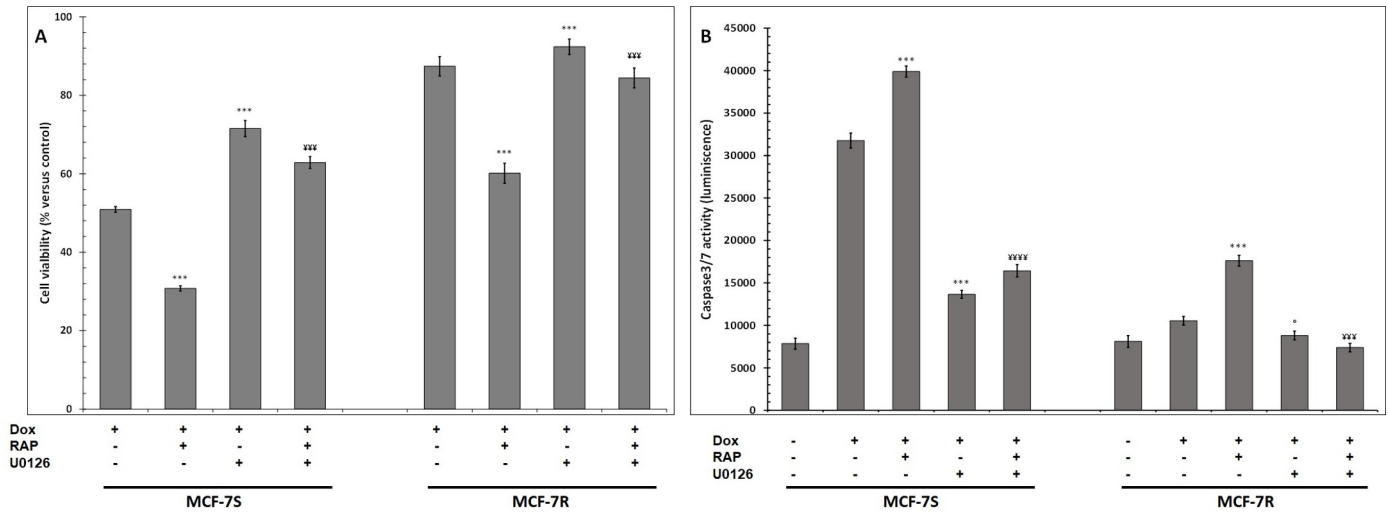
Fig 10. ERK1/2 inhibition reduced Dox cytotoxic effects on MCF-7 cells. MCF-7S and MCF-7R cells were incubated with 1 µM Dox with or without 500 nM RAP and 1 µM U0126 48 hours. **A**, Cell viability was measured using UptiBlue Viable Cell Assay. **B**, Caspase-7 activity was measured by caspACE assay kit. The results obtained from three independent experiments (% of control) were represented with standard deviation (S.D.). Student's t-test was used for the statistical significance of different values. *** $p < 0.001$ compared to Dox-treated cells and ¥¥¥ $p < 0.001$, ¥¥¥¥ $p < 0.0001$ compared to Dox- and RAP-treated cells.˚ NS, U0126-treated cells versus Dox-treated cells.

study, the decrease of LAMP-1 suggested the removal of this protection which could lead to the degradation of P-gp and consequently a decrease of its level at the cellular level. This would support the hypothesis that LAMP-1 was involved in the modulation of P-gp-induced Dox resistance in MCF-7R cells.

Dox-induced apoptosis has been largely described as involving activation of the MAP kinases ERK 1/2 and the caspase 3 in different cell types. In this study, we showed that, in MCF-7 parental cells, Dox involved ERK 1/2 phosphorylation in apoptosis induction. In fact, ERK 1/2 inhibition markedly suppressed the Dox pro-apoptotic effect. Several studies
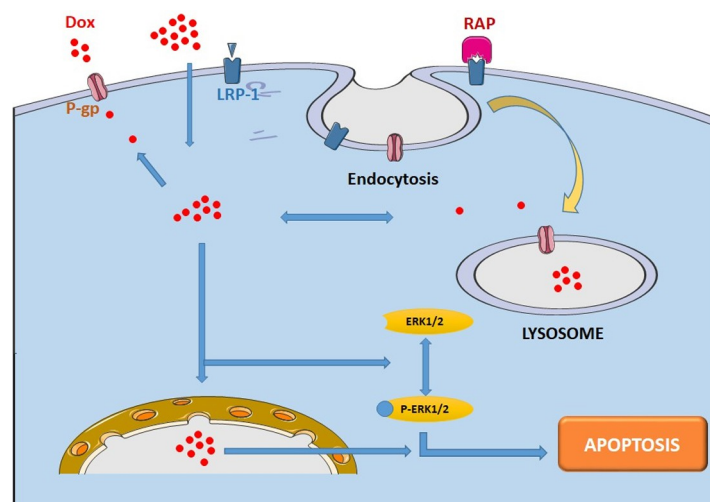
Fig 11. Schematic diagram of P-gp internalization by LRP-1 receptor and its implication in MCF-7 cells drug resistance.

confirmed the implication of ERK1/2 apoptosis activation via the enhancement of Fas ligand expression and the inactivation of BAD, a member of the pro-apoptotic bcl-2 family [76, 77].

Interestingly, in MCF-7 resistant cells characterized by a high P-gp level expression, ERK 1/ 2 are not activated leading to a resistance to Dox. LRP-1 blockade promoted ERK 1/2 activation and sensitized MCF-7 resistant cells to Dox.

The only publication showing a link between endosomes and ERK1/2 via the p14/MP1 complex was reported by Teis et al. [78]. In MCF-7 cells, MP1 was not detected by Western blot.

Thus, our data suggest that LRP-1 is able to modulate ERK1/2 signaling pathway by regulating expression and subcellular redistribution of P-gp and by potentializing the P-gp-acquired Dox resistance Fig 11.

Some previous studies have indicated that several survival-related or death-associated signaling pathways, including the PI-3K/Akt and MAPKs pathways, play pivotal roles in the regulation of DNA damage-induced apoptosis [79–83]. Thus, pharmacological modulation of MAPK signaling has been determined to influence apoptotic responses to these anti-cancer drugs. However, the role played by MAPKs depends on cell type and drug concentration [84]. Activation of the ERK 1/2 pathway is generally associated to cell proliferation and/or survival. However, the ERK1/2 pathway can also stimulate apoptosis [85–87].

Our study showed that P-gp was present in both plasma membrane and lysosomes of MCF-7 resistant cells. P-gp internalization was controlled by LRP-1 *via* an endocytic traffic, suggesting that LRP-1 contributed to lysosomal trafficking of P-gp and consequently controlled the P-gp acquired-resistance of MCF-7 cells to Dox. Previous studies have confirmed that P-gp is functional on the plasma membrane and in lysosomes. Lysosomal P-gp increased the trapping of Dox, preventing it from reaching its targets, and conferred drug resistance. This resistance can be circumvented by lysosomotropic agents that can induce increased Dox cytotoxicity. [20, 88].

While the canonical mechanism of P-gp action is mediated by its localization and activity at the plasma membrane, the role of intracellular P-gp may be crucial to consider in drug therapy [68]. Our study reported that intracellular P-gp-mediated sequestration of the drug in lysosomes could serve as an additional mechanism to drug efflux *via* plasma membrane-bound P-gp for multidrug-resistance. Several studies been demonstrated that P-gp not only functions to efflux drugs out of the cell when present on the plasma membrane but also serves a functional intracellular role in the lysosomal membrane to induce resistance [20]. This mechanism may be exploitable with combination therapy to overcome intracellular MDR. Indeed, classical lysosomotropic agents, such as chloroquine, in combination with current ineffective drug treatments for MDR, could cause the lysosomal-release of these agents to increase their chances of reaching sensitive intracellular targets and regain efficacy [20, 89]. Inhibition of P-gp internalization by blocking LRP-1 could offer a fruitful new strategy to enhance lysosomal accumulation of cytotoxic drugs and serve as a new target and an alternative strategy to effectively battle multidrug-resistance.

Acknowledgments

Author Contributions

Conceptualization: Laurent Martiny, Hassan El Btaouri.

Investigation: Aubery Henry, Marine Mauperin, Jerome Devy, Stephane Dedieu, Lise Chazee, Cathy Hachet, Christine Terryn, Laurent Duca, Laurent Martiny, Emmanuelle Devarenne-Charpentier, Hassan El Btaouri.

Project administration: Hassan El Btaouri.

Supervision: Laurent Martiny.

Writing – original draft: Emmanuelle Devarenne-Charpentier, Hassan El Btaouri.

References

1. Aleksakhina S.N., Kashyap A., Imyanitov E.N., Mechanisms of acquired tumor drug resistance, Biochimica et biophysica acta. Reviews on cancer, 1872 (2019) 188310.

2. Harrison D.J., Molecular mechanisms of drug resistance in tumours, The Journal of pathology, 175 (1995) 7–12. https://doi.org/10.1002/path.1711750103 PMID: 7891229

3. Longley D.B., Johnston P.G., Molecular mechanisms of drug resistance, The Journal of pathology, (2005) 275–292. https://doi.org/10.1002/path.1706 PMID: 15641020

4. Denkert C., Loibl S., Noske A., Roller M., Muller B.M., Komor M., et al, Tumor-associated lymphocytes as an independent predictor of response to neoadjuvant chemotherapy in breast cancer, Journal of clinical oncology: official journal of the American Society of Clinical Oncology, 28 (2010) 105–113.

5. Mattarollo S.R., Loi S., Duret H., Ma Y., Zitvogel L., Smyth M.J., Pivotal role of innate and adaptive immunity in anthracycline chemotherapy of established tumors, Cancer research, 71 (2011) 4809–4820. https://doi.org/10.1158/0008-5472.CAN-11-0753 PMID: 21646474

6. Pitt J.M., Vetizou M., Daillere R., Roberti M.P., Yamazaki T., Routy B., et al, Resistance Mechanisms to Immune-Checkpoint Blockade in Cancer: Tumor-Intrinsic and -Extrinsic Factors, Immunity, 44 (2016) 1255–1269. https://doi.org/10.1016/j.immuni.2016.06.001 PMID: 27332730

7. Sharma P., Hu-Lieskovan S., Wargo J.A., Ribas A., Primary, Adaptive, and Acquired Resistance to Cancer Immunotherapy, Cell, 168 (2017) 707–723. https://doi.org/10.1016/j.cell.2017.01.017 PMID: 28187290

8. O'Donnell J.S., Long G.V., Scolyer R.A., Teng M.W., Smyth M.J., Resistance to PD1/PDL1 checkpoint inhibition, Cancer treatment reviews, 52 (2017) 71–81. https://doi.org/10.1016/j.ctrv.2016.11.007 PMID: 27951441

9. Hoshiba T., An extracellular matrix (ECM) model at high malignant colorectal tumor increases chondroitin sulfate chains to promote epithelial-mesenchymal transition and chemoresistance acquisition, Experimental cell research, 370 (2018) 571–578. https://doi.org/10.1016/j.yexcr.2018.07.022 PMID: 30016638

10. Hazlehurst L.A., Argilagos R.F., Emmons M., Boulware D., Beam C.A., Sullivan D.M., et al, Cell adhesion to fibronectin (CAM-DR) influences acquired mitoxantrone resistance in U937 cells, Cancer research, 66 (2006) 2338–2345. https://doi.org/10.1158/0008-5472.CAN-05-3256 PMID: 16489039

11. Naci D., El Azreq M.-A., Chetoui N., Lauden L., Sigaux F., Charron D., et al, alpha2beta1 integrin promotes chemoresistance against doxorubicin in cancer cells through extracellular signal-regulated kinase (ERK), The Journal of biological chemistry, 287 (2012) 17065–17076.

12. Aoudjit F., Vuori K., Integrin signaling inhibits paclitaxel-induced apoptosis in breast cancer cells, Oncogene, 20 (2001) 4995–5004. https://doi.org/10.1038/sj.onc.1204554 PMID: 11526484

13. Courageot M.P., Duca L., Martiny L., Devarenne-Charpentier E., Morjani H., El Btaouri H., Thrombospondin-1 Receptor CD47 Overexpression Contributes to P-Glycoprotein-Mediated Multidrug Resistance Against Doxorubicin in Thyroid Carcinoma FTC-133 Cells, Frontiers in oncology, 10 (2020) 551228. https://doi.org/10.3389/fonc.2020.551228 PMID: 33365267

14. Fletcher J.I., Williams R.T., Henderson M.J., Norris M.D., Haber M., ABC transporters as mediators of drug resistance and contributors to cancer cell biology, Drug resistance updates: reviews and commentaries in antimicrobial and anticancer chemotherapy, 26 (2016) 1–9.

15. Dean M., The genetics of ATP-binding cassette transporters, Methods in enzymology, 400 (2005) 409–429. https://doi.org/10.1016/S0076-6879(05)00024-8 PMID: 16399363

16. Deeley R.G., Westlake C., Cole S.P., Transmembrane transport of endo- and xenobiotics by mammalian ATP-binding cassette multidrug resistance proteins, Physiological reviews, 86 (2006) 849–899. https://doi.org/10.1152/physrev.00035.2005 PMID: 16816140

17. Fu D., Arias I.M., Intracellular trafficking of P-glycoprotein, The international journal of biochemistry & cell biology, 44 (2012) 461–464. https://doi.org/10.1016/j.biocel.2011.12.009 PMID: 22212176

18. Fu D., Bebawy M., Kable E.P., Roufogalis B.D., Dynamic and intracellular trafficking of P-glycoprotein-EGFP fusion protein: Implications in multidrug resistance in cancer, International journal of cancer, 109 (2004) 174–181. https://doi.org/10.1002/ijc.11659 PMID: 14750166

19. Fu D., Roufogalis B.D., Actin disruption inhibits endosomal traffic of P-glycoprotein-EGFP and resistance to daunorubicin accumulation, American journal of physiology. Cell physiology, 292 (2007) C1543–1552.

20. Yamagishi T., Sahni S., Sharp D.M., Arvind A., Jansson P.J., Richardson D.R., P-glycoprotein mediates drug resistance via a novel mechanism involving lysosomal sequestration, The Journal of biological chemistry, 288 (2013) 31761–31771. https://doi.org/10.1074/jbc.M113.514091 PMID: 24062304

21. Endicott J.A., Ling V., The biochemistry of P-glycoprotein-mediated multidrug resistance, Annual review of biochemistry, 58 (1989) 137–171. https://doi.org/10.1146/annurev.bi.58.070189.001033 PMID: 2570548

22. Higgins C.F., Multiple molecular mechanisms for multidrug resistance transporters, Nature, 446 (2007) 749–757. https://doi.org/10.1038/nature05630 PMID: 17429392

23. Nykjaer A., Willnow T.E., The low-density lipoprotein receptor gene family: a cellular Swiss army knife?, Trends in cell biology, 12 (2002) 273–280. https://doi.org/10.1016/s0962-8924(02)02282-1 PMID: 12074887

24. Strickland D.K., Gonias S.L., Argraves W.S., Diverse roles for the LDL receptor family, Trends in endocrinology and metabolism: TEM, 13 (2002) 66–74.

25. Willnow T.E., The low-density lipoprotein receptor gene family: multiple roles in lipid metabolism, Journal of molecular medicine, 77 (1999) 306–315. https://doi.org/10.1007/s001090050356 PMID: 10090593

26. Andre S., Larbanoix L., Verteneuil S., Stanicki D., Nonclercq D., Vander Elst L., et al. Burtea, Development of an LDL Receptor-Targeted Peptide Susceptible to Facilitate the Brain Access of Diagnostic or Therapeutic Agents, Biology, 9 (2020).

27. Barcelona P.F., Luna J.D., Chiabrando G.A., Juarez C.P., Bhutto I.A., Baba T., et al, Immunohistochemical localization of low density lipoprotein receptor-related protein 1 and alpha(2)-Macroglobulin in retinal and choroidal tissue of proliferative retinopathies, Experimental eye research, 91 (2010) 264–272. https://doi.org/10.1016/j.exer.2010.05.017 PMID: 20561980

28. Ferrer D.G., Jaldin-Fincati J.R., Amigone J.L., Capra R.H., Collino C.J., Albertini R.A., et al, Standardized flow cytometry assay for identification of human monocytic heterogeneity and LRP1 expression in monocyte subpopulations: decreased expression of this receptor in nonclassical monocytes, Cytometry. Part A: the journal of the International Society for Analytical Cytology, 85 (2014) 601–610.

29. Gonias S.L., Campana W.M., LDL receptor-related protein-1: a regulator of inflammation in atherosclerosis, cancer, and injury to the nervous system, The American journal of pathology, 184 (2014) 18–27. https://doi.org/10.1016/j.ajpath.2013.08.029 PMID: 24128688

30. Boucher P., Herz J., Signaling through LRP1: Protection from atherosclerosis and beyond, Biochemical pharmacology, 81 (2011) 1–5. https://doi.org/10.1016/j.bcp.2010.09.018 PMID: 20920479

31. Gonias S.L., Gaultier A., Jo M., Regulation of the urokinase receptor (uPAR) by LDL receptor-related protein-1 (LRP1), Current pharmaceutical design, 17 (2011) 1962–1969. https://doi.org/10.2174/138161211796718224 PMID: 21711236

32. Pi X., Schmitt C.E., Xie L., Portbury A.L., Wu Y., Lockyer P., et al, LRP1-dependent endocytic mechanism governs the signaling output of the bmp system in endothelial cells and in angiogenesis, Circulation research, 111 (2012) 564–574. https://doi.org/10.1161/CIRCRESAHA.112.274597 PMID: 22777006

33. Rabiej V.K., Pflanzner T., Wagner T., Goetze K., Storck S.E., Eble J.A., et al, Low density lipoprotein receptor-related protein 1 mediated endocytosis of beta1-integrin influences cell adhesion and cell migration, Experimental cell research, 340 (2016) 102–115.

34. Capurro M.I., Shi W., Filmus J., LRP1 mediates Hedgehog-induced endocytosis of the GPC3-Hedgehog complex, Journal of cell science, 125 (2012) 3380–3389. https://doi.org/10.1242/jcs.098889 PMID: 22467855

35. Gonias S.L., Wu L., Salicioni A.M., Low density lipoprotein receptor-related protein: regulation of the plasma membrane proteome, Thrombosis and haemostasis, 91 (2004) 1056–1064. https://doi.org/10.1160/TH04-01-0023 PMID: 15175790

36. Langlois B., Perrot G., Schneider C., Henriet P., Emonard H., Martiny L., et al LRP-1 promotes cancer cell invasion by supporting ERK and inhibiting JNK signaling pathways, PloS one, 5 (2010) e11584.

37. Chazaud B., Ricoux R., Christov C., Plonquet A., Gherardi R.K., Barlovatz-Meimon G., Promigratory effect of plasminogen activator inhibitor-1 on invasive breast cancer cell populations, The American journal of pathology, 160 (2002) 237–246. https://doi.org/10.1016/S0002-9440(10)64367-2 PMID: 11786417

38. Fayard B., Bianchi F., Dey J., Moreno E., Djaffer S., Hynes N.E., et al, The serine protease inhibitor protease nexin-1 controls mammary cancer metastasis through LRP-1-mediated MMP-9 expression,

Cancer research, 69 (2009) 5690–5698. https://doi.org/10.1158/0008-5472.CAN-08-4573 PMID: 19584287

39. Montel V., Gaultier A., Lester R.D., Campana W.M., Gonias S.L., The low-density lipoprotein receptor-related protein regulates cancer cell survival and metastasis development, Cancer research, 67 (2007) 9817–9824. https://doi.org/10.1158/0008-5472.CAN-07-0683 PMID: 17942912

40. Martinez-Ledesma E., Verhaak R.G., Trevino V., Identification of a multi-cancer gene expression bio-marker for cancer clinical outcomes using a network-based algorithm, Scientific reports, 5 (2015) 11966. https://doi.org/10.1038/srep11966 PMID: 26202601

41. Perrot G., Langlois B., Devy J., Jeanne A., Verzeaux L., Almagro S., et al LRP-1—CD44, a new cell surface complex regulating tumor cell adhesion, Molecular and cellular biology, 32 (2012) 3293–3307.

42. Appert-Collin A., Bennasroune A., Jeannesson P., Terryn C., Fuhrmann G., Morjani H., et al, Role of LRP-1 in cancer cell migration in 3-dimensional collagen matrix, Cell adhesion & migration, 11 (2017) 316–326. https://doi.org/10.1080/19336918.2016.1215788 PMID: 27463962

43. Chen J., Wei H., Cheng J., Xie B., Wang B., Yi J., et al B., Characteristics of doxorubicin-selected multi-drug-resistant human leukemia HL-60 cells with tolerance to arsenic trioxide and contribution of leuke-mia stem cells, Oncology letters, 15 (2018) 1255–1262. https://doi.org/10.3892/ol.2017.7353 PMID: 29399180

44. Morjani H., Millot J.M., Belhoussine R., Sebille S., Manfait M., Anthracycline subcellular distribution in human leukemic cells by microspectrofluorometry: factors contributing to drug-induced cell death and reversal of multidrug resistance, Leukemia, 11 (1997) 1170–1179. https://doi.org/10.1038/sj.leu.2400668 PMID: 9205008

45. de Araujo M.E., Lamberti G., Huber L.A., Isolation of Early and Late Endosomes by Density Gradient Centrifugation, Cold Spring Harbor protocols, 2015 (2015) 1013–1016. https://doi.org/10.1101/pdb.prot083444 PMID: 26527762

46. Gusakov A.V., Kondratyeva E.G., Sinitsyn A.P., Comparison of two methods for assaying reducing sug-ars in the determination of carbohydrase activities, International journal of analytical chemistry, 2011 (2011) 283658. https://doi.org/10.1155/2011/283658 PMID: 21647284

47. Fairchild C.R., Ivy S.P., Kao-Shan C.S., Whang-Peng J., Rosen N., Israel M.A., et al, Isolation of ampli-fied and overexpressed DNA sequences from adriamycin-resistant human breast cancer cells, Cancer research, 47 (1987) 5141–5148. PMID: 2441861

48. Rath G.M., Schneider C., Dedieu S., Rothhut B., Soula-Rothhut M., Ghoneim C., et al, The C-terminal CD47/IAP-binding domain of thrombospondin-1 prevents camptothecin- and doxorubicin-induced apo-ptosis in human thyroid carcinoma cells, Biochimica et biophysica acta, 1763 (2006) 1125–1134. https://doi.org/10.1016/j.bbamcr.2006.08.001 PMID: 16962673

49. Janicke R.U., MCF-7 breast carcinoma cells do not express caspase-3, Breast cancer research and treatment, 117 (2009) 219–221. https://doi.org/10.1007/s10549-008-0217-9 PMID: 18853248

50. Fu D., van Dam E.M., Brymora A., Duggin I.G., Robinson P.J., Roufogalis B.D., The small GTPases Rab5 and RalA regulate intracellular traffic of P-glycoprotein, Biochimica et biophysica acta, 1773 (2007) 1062–1072. https://doi.org/10.1016/j.bbamcr.2007.03.023 PMID: 17524504

51. Kim H., Barroso M., Samanta R., Greenberger L., Sztul E., Experimentally induced changes in the endocytic traffic of P-glycoprotein alter drug resistance of cancer cells, The American journal of physiol-ogy, 273 (1997) C687–702. https://doi.org/10.1152/ajpcell.1997.273.2.C687 PMID: 9277367

52. Katayama K., Noguchi K., Sugimoto Y., FBXO15 regulates P-glycoprotein/ABCB1 expression through the ubiquitin—proteasome pathway in cancer cells, Cancer science, 104 (2013) 694–702. https://doi.org/10.1111/cas.12145 PMID: 23465077

53. Lee E.R., Kim J.Y., Kang Y.J., Ahn J.Y., Kim J.H., Kim B.W., et al, Interplay between PI3K/Akt and MAPK signaling pathways in DNA-damaging drug-induced apoptosis, Biochimica et biophysica acta, 1763 (2006) 958–968. https://doi.org/10.1016/j.bbamcr.2006.06.006 PMID: 16905201

54. Juliano R.L., The role of drug delivery systems in cancer chemotherapy, Progress in clinical and biologi-cal research, 9 (1976) 21–32. PMID: 1030801

55. Nanayakkara A.K., Follit C.A., Chen G., Williams N.S., Vogel P.D., Wise J.G., Targeted inhibitors of P-glycoprotein increase chemotherapeutic-induced mortality of multidrug resistant tumor cells, Scientific reports, 8 (2018) 967. https://doi.org/10.1038/s41598-018-19325-x PMID: 29343829

56. Campos L., Guyotat D., Archimbaud E., Calmard-Oriol P., Tsuruo T., Troncy J., et al, Clinical signifi-cance of multidrug resistance P-glycoprotein expression on acute nonlymphoblastic leukemia cells at diagnosis, Blood, 79 (1992) 473–476. PMID: 1370388

57. Marie J.P., Zittoun R., Sikic B.I., Multidrug resistance (mdr1) gene expression in adult acute leukemias: correlations with treatment outcome and in vitro drug sensitivity, Blood, 78 (1991) 586–592. PMID: 1859877

58. Seebacher N., Lane D.J., Richardson D.R., Jansson P.J., Turning the gun on cancer:Utilizing lysosomal P-glycoprotein as a new strategy to overcome multi-drug resistance, Free radical biology & medicine, (2016) 432–445. https://doi.org/10.1016/j.freeradbiomed.2016.04.201 PMID: 27154979

59. Seebacher N.A., Lane D.J., Jansson P.J., Richardson D.R., Glucose Modulation Induces Lysosome Formation and Increases Lysosomotropic Drug Sequestration via the P-Glycoprotein Drug Transporter, The Journal of biological chemistry, 291 (2016) 3796–3820. https://doi.org/10.1074/jbc.M115.682450 PMID: 26601947

60. Kanekiyo T., Bu G., The low-density lipoprotein receptor-related protein 1 and amyloid-beta clearance in Alzheimer's disease, Frontiers in aging neuroscience, 6 (2014) 93.

61. Li Y., Marzolo M.P., van Kerkhof P., Strous G.J., Bu G., The YXXL motif, but not the two NPXY motifs, serves as the dominant endocytosis signal for low density lipoprotein receptor-related protein, The Journal of biological chemistry, 275 (2000) 17187–17194. https://doi.org/10.1074/jbc.M000490200 PMID: 10747918

62. Dehay B., Bove J., Rodriguez-Muela N., Perier C., Recasens A., Boya P., et al, Pathogenic lysosomal depletion in Parkinson's disease, The Journal of neuroscience: the official journal of the Society for Neuroscience, 30 (2010) 12535–12544.

63. Kundra R., Kornfeld S., Asparagine-linked oligosaccharides protect Lamp-1 and Lamp-2 from intracellular proteolysis, The Journal of biological chemistry, 274 (1999) 31039–31046. https://doi.org/10.1074/jbc.274.43.31039 PMID: 10521503

64. Fehrenbacher N., Bastholm L., Kirkegaard-Sorensen T., Rafn B., Bottzauw T., Nielsen C., et al. Jaattela, Sensitization to the lysosomal cell death pathway by oncogene-induced down-regulation of lysosome-associated membrane proteins 1 and 2, Cancer research, 68 (2008) 6623–6633.

65. Furuta K., Ikeda M., Nakayama Y., Nakamura K., Tanaka M., Hamasaki N., et al. August, Expression of lysosome-associated membrane proteins in human colorectal neoplasms and inflammatory diseases, The American journal of pathology, 159 (2001) 449–455.

66. Ozaki K., Nagata M., Suzuki M., Fujiwara T., Ueda K., Miyoshi Y., et al, Isolation and characterization of a novel human lung-specific gene homologous to lysosomal membrane glycoproteins 1 and 2: significantly increased expression in cancers of various tissues, Cancer research, 58 (1998) 3499–3503. PMID: 9721848

67. Wang Q., Yao J., Jin Q., Wang X., Zhu H., Huang F., et al, LAMP1 expression is associated with poor prognosis in breast cancer, Oncology letters, 14 (2017) 4729–4735. https://doi.org/10.3892/ol.2017.6757 PMID: 29085473

68. Geisslinger F., Muller M., Vollmar A.M., Bartel K., Targeting Lysosomes in Cancer as Promising Strategy to Overcome Chemoresistance-A Mini Review, Frontiers in oncology, 10 (2020) 1156. https://doi.org/10.3389/fonc.2020.01156 PMID: 32733810

69. Fassl A., Brain C., Abu-Remaileh M., Stukan I., Butter D., Stepien P., et al. Sicinski, Increased lysosomal biomass is responsible for the resistance of triple-negative breast cancers to CDK4/6 inhibition, Science advances, 6 (2020) eabb2210.

70. Krishnan V., Bane S.M., Kawle P.D., Naresh K.N., Kalraiya R.D., Altered melanoma cell surface glycosylation mediates organ specific adhesion and metastasis via lectin receptors on the lung vascular endothelium, Clinical & experimental metastasis, 22 (2005) 11–24. https://doi.org/10.1007/s10585-005-2036-2 PMID: 16132574

71. Zhitomirsky B., Assaraf Y.G., Lysosomes as mediators of drug resistance in cancer, Drug resistance updates: reviews and commentaries in antimicrobial and anticancer chemotherapy, 24 (2016) 23–33.

72. Fukuda M., Lysosomal membrane glycoproteins. Structure, biosynthesis, and intracellular trafficking, The Journal of biological chemistry, 266 (1991) 21327–21330.

73. Kornfeld S., Mellman I., The biogenesis of lysosomes, Annual review of cell biology, 5 (1989) 483–525. https://doi.org/10.1146/annurev.cb.05.110189.002411 PMID: 2557062

74. Neiss W.F., A coat of glycoconjugates on the inner surface of the lysosomal membrane in the rat kidney, Histochemistry, 80 (1984) 603–608. PMID: 6469717

75. Sawada R., Jardine K.A., Fukuda M., The genes of major lysosomal membrane glycoproteins, lamp-1 and lamp-2. 5'-flanking sequence of lamp-2 gene and comparison of exon organization in two genes, The Journal of biological chemistry, 268 (1993) 9014–9022. PMID: 8517882

76. Basu S., Bayoumy S., Zhang Y., Lozano J., Kolesnick R., BAD enables ceramide to signal apoptosis via Ras and Raf-1, The Journal of biological chemistry, 273 (1998) 30419–30426. https://doi.org/10.1074/jbc.273.46.30419 PMID: 9804808

77. van den Brink M.R., Kapeller R., Pratt J.C., Chang J.H., Burakoff S.J., The extracellular signal-regulated kinase pathway is required for activation-induced cell death of T cells, The Journal of biological chemistry, 274 (1999) 11178–11185. https://doi.org/10.1074/jbc.274.16.11178 PMID: 10196203

78. Teis D., Wunderlich W., Huber L.A., Localization of the MP1-MAPK scaffold complex to endosomes is mediated by p14 and required for signal transduction, Developmental cell, 3 (2002) 803–814. https://doi.org/10.1016/s1534-5807(02)00364-7 PMID: 12479806

79. El Btaouri H., Morjani H., Greffe Y., Charpentier E., Martiny L., Role of JNK/ATF-2 pathway in inhibition of thrombospondin-1 (TSP-1) expression and apoptosis mediated by doxorubicin and camptothecin in FTC-133 cells, Biochimica et biophysica acta, 1813 (2011) 695–703. https://doi.org/10.1016/j.bbamcr.2011.02.004 PMID: 21333695

80. Guise S., Braguer D., Carles G., Delacourte A., Briand C., Hyperphosphorylation of tau is mediated by ERK activation during anticancer drug-induced apoptosis in neuroblastoma cells, Journal of neuroscience research, 63 (2001) 257–267. https://doi.org/10.1002/1097-4547(20010201)63:3<257::AID-JNR1019>3.0.CO;2-T PMID: 11170175

81. Kang Y.J., Zhou Z.X., Wang G.W., Buridi A., Klein J.B., Suppression by metallothionein of doxorubicin-induced cardiomyocyte apoptosis through inhibition of p38 mitogen-activated protein kinases, The Journal of biological chemistry, 275 (2000) 13690–13698. https://doi.org/10.1074/jbc.275.18.13690 PMID: 10788488

82. Negoro S., Oh H., Tone E., Kunisada K., Fujio Y., Walsh K., et al, Glycoprotein 130 regulates cardiac myocyte survival in doxorubicin-induced apoptosis through phosphatidylinositol 3-kinase/Akt phosphorylation and Bcl-xL/caspase-3 interaction, Circulation, 103 (2001) 555–561. https://doi.org/10.1161/01.cir.103.4.555 PMID: 11157722

83. Yu R., Shtil A.A., Tan T.H., Roninson I.B., Kong A.N., Adriamycin activates c-jun N-terminal kinase in human leukemia cells: a relevance to apoptosis, Cancer letters, 107 (1996) 73–81. https://doi.org/10.1016/0304-3835(96)04345-5 PMID: 8913269

84. Fan M., Chambers T.C., Role of mitogen-activated protein kinases in the response of tumor cells to chemotherapy, Drug resistance updates: reviews and commentaries in antimicrobial and anticancer chemotherapy, 4 (2001) 253–267. https://doi.org/10.1054/drup.2001.0214 PMID: 11991680

85. Cagnol S., Chambard J.C., ERK and cell death: mechanisms of ERK-induced cell death—apoptosis, autophagy and senescence, The FEBS journal, 277 (2010) 2–21. https://doi.org/10.1111/j.1742-4658.2009.07366.x PMID: 19843174

86. Kole L., Sarkar M., Deb A., Giri B., Pioglitazone, an anti-diabetic drug requires sustained MAPK activation for its anti-tumor activity in MCF7 breast cancer cells, independent of PPAR-gamma pathway, Pharmacological reports: PR, 68 (2016) 144–154.

87. Yahiro K., Hirayama T., Moss J., Noda M., Helicobacter pylori VacA toxin causes cell death by inducing accumulation of cytoplasmic connexin 43, Cell death & disease, 6 (2015) e1971.

88. Halaby R., Influence of lysosomal sequestration on multidrug resistance in cancer cells, Cancer drug resistance, 2 (2019) 31–42. https://doi.org/10.20517/cdr.2018.23 PMID: 35582144

89. Styrt B., Klempner M.S., Inhibition of neutrophil oxidative metabolism by lysosomotropic weak bases, Blood, 67 (1986) 334–342. PMID: 3002523